Auditory nerve fiber modeling: A stochastic Melnikov approach

Marek Franaszek* and Emil Simiu
Building and Fire Research Laboratory, Building 226, National Institute of Standards and Technology, Gaithersburg, Maryland 20899
(Received 5 December 1996; revised manuscript received 1 December 1997)

Well-known experiments have established two basic features of auditory nerve fiber dynamics. First, harmonic excitation with constant amplitude produces mean firing rates that are largest for excitation frequencies contained in a relatively narrow best interval; for frequencies outside that interval mean firing rates decrease until, for both low and high frequencies, they become vanishingly small. Second, white or nearly white noise excitation results in multimodal interspike interval histograms. These features suggested the development of a strongly asymmetrical bistable model to which Melnikov theory applies. We show that, unlike the Fitzhugh-Nagumo equation, such a model is capable of reproducing both basic features of the dynamics. We also show that the model is consistent with experimental results on response patterns for excitation by two harmonics in the presence of spontaneous activity. The Melnikov properties of the proposed model explain both its qualitatively satisfactory performance and its potential for stochastic resonant behavior. Numerical tests confirm the robustness of the proposed model. [S1063-651X(98)03304-2]

PACS number(s): 87.10.+e, 05.40.+j, 05.45.+b

I. INTRODUCTION

The auditory nerve fiber is a device of interest to both neurophysiologists and signal processing engineers. Experiments have established two basic features of its dynamics. First, mean firing rates produced by harmonic excitation in the presence of weak noise are largest for excitation frequencies contained in a relatively narrow best interval; for frequencies outside that interval mean firing rates decrease and, for both low and high frequencies, become vanishingly small [1] (Fig. 1). Second, white or nearly white noise excitation results in multimodal interspike interval histograms (ISIH's) with modes approximately equal to integer multiples of the period corresponding to the nerve fiber's best frequency [2] (Fig. 2).

The Fitzhugh-Nagumo (FHN) model appears to be unable to reproduce these two dynamical features. According to [3], in the absence of noise the FHN model predicts correctly that, as the excitation frequency increases beyond the best frequencies, the amplitude of the harmonic signal needed to cause firing increases sharply. However, the model fails to predict a similarly sharp increase for excitation frequencies lower than the best frequencies (Fig. 3). In the presence of noise the disagreement between typical FHN model predictions and the experimental results of [1] appears to be even stronger; see Ref. [3], p. 561. Also, according to [4], for nearly white noise excitation the FHN model yields a unimodal ISIH (Fig. 4), in disagreement with the experimental results of [2].

We propose a dynamical model consisting of an asymmetric bistable damped forced one-degree-of-freedom oscillator whose undamped, unforced counterpart has homoclinic orbits. A nerve fiber firing corresponds in this model to an escape from a potential well. We show that, in contrast to the FHN model, our model reproduces the experimentally observed dynamical features noted earlier. The model is also consistent with experimental results on response patterns for excitation by two harmonics in the presence of spontaneous activity. Our model belongs to the wide class of systems to which Melnikov theory is applicable [5–7]. Its performance can be interpreted transparently in terms of that theory, which is also applicable to the investigation of the model's potential for stochastic resonant behavior, a phenomenon that has been shown recently to be significant for the transmission of information by certain types of neuronal systems [8]. The ability of the proposed model to reproduce qualitatively dynamic behavior under predominantly harmonic or quasiperiodic forcing or under stochastic forcing is due to the following basic properties of a wide class of bistable one-degree-of-freedom oscillators subjected to harmonic forcing: (i) For any fixed excitation frequency, there exists a range of excitation amplitudes for which the mean escape rate increases as the excitation amplitude increases and (ii) for any fixed excitation amplitude within that range, there exists a ''best'' frequency for which the mean escape rate is largest and mean escape rates decrease monotonically as the absolute value of the difference between the excitation frequency and the best frequency increases [5]. We verify in this paper that these properties are robust.

We describe the proposed model in Sec. II. In Sec. III we review briefly relevant results of Melnikov theory and show that, in view of the experiments of [1], the proposed model is suggested naturally by those results. In Sec. IV we discuss the model's chaotic motion and its ability to reproduce the firing behavior of the auditory nerve fiber. In Sec. V we illustrate the model's ability, inherent in its Melnikov properties, to reproduce qualitatively the dependence on the frequency and amplitude of a harmonic excitation's effectiveness in causing firing (escapes). In Secs. IV and V we also discuss the model's robustness. In Sec. VI we show that, for the proposed model, excitation by white noise results in multimodal ISIH's, in agreement with experiment. We also discuss a set of experimental results obtained under excitation by a sum of two harmonics in the presence of spontaneous

*Permanent address: Institute of Physics, Cracow Pedagogical University, Podchorążych 2, Kraków, Poland.

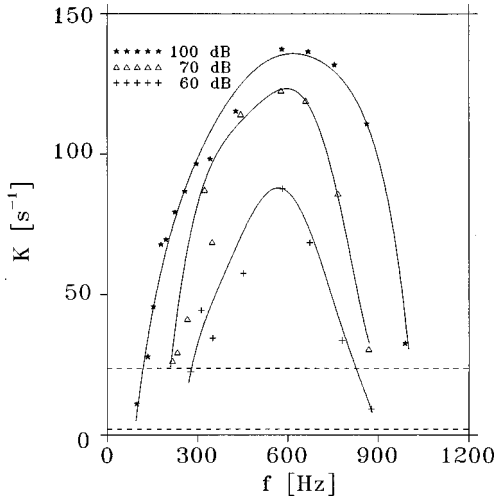

FIG. 1. Dependence of the mean firing rate K on frequency and amplitude of harmonic excitation (after [1] where $T_{tot}=20$ s). ($K=Q/T_{tot}$, where Q is the total number of spikes observed in time T_{tot} for harmonically excited auditory nerve fiber in a squirrel monkey.) Dashed lines indicate levels of spontaneous firing.

activity and show that our model is consistent with those results. Section VII notes the relation between the model's Melnikov properties and its potential for stochastic resonant behavior. Section VIII presents our conclusions.

II. ASYMMETRIC BISTABLE MODEL OF AUDITORY NERVE FIBER RESPONSE

We model the response of the auditory nerve fiber by the nondimensional equation

$$\ddot{x}=-V'(x)+\varepsilon(x)\times[\gamma_{01}\cos(\omega_{01}t)+\gamma_{02}\cos(\omega_{02}t)+\sigma G(t)-\beta\dot{x}], \tag{1}$$

where

$$\varepsilon(x)\equiv 1-H(x). \tag{2}$$

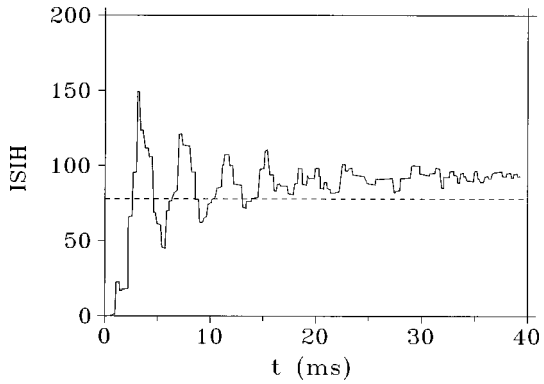

FIG. 2. Interspike interval histogram for response to white noise of auditory nerve fiber in a squirrel monkey (after [2]). The interrupted line indicates the level of the spontaneous firing rate. Modes are approximately equal to integer multiples of the period corresponding to the fiber's best frequency.

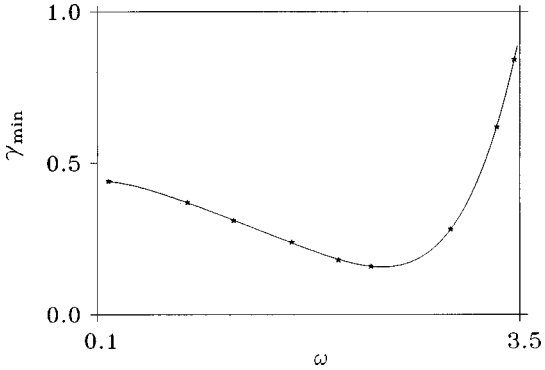

FIG. 3. Dependence of the minimum amplitude needed to produce firings γ_{min} on the frequency of the harmonic excitation in the absence of noise, as modeled by the Fitzhugh-Nagumo equation (after [3]). The horizontal scale is logarithmic.

$H(x)$ is the unit step (Heaviside) function. The dimensional counterparts of the variable x and of typical excitation terms are discussed in the Appendix. β is a damping parameter and $V(x)$ is a potential function. We need expressions for $V(x)$ and values of the parameter β such that, under excitation by stimuli matching those reported in experiments, Eq. (1) yield responses matching the observed behavior. In addition, it is necessary to ascertain that Eq. (1) is a robust system (alternative terms are ''coarse system'' or ''structurally stable system'').

The unperturbed counterpart of Eq. (1) is the Hamiltonian system

$$\ddot{x}=-V'(x). \tag{3}$$

We assume that $V(x)$ is a double-well potential with a barrier whose maximum occurs at $x=0$ [Fig. 5(a)]. Because motions with firings are asymmetrical, we also assume that the potential is asymmetrical [Fig. 5(b)].

Equation (3) has a hyperbolic fixed point at the origin. Emerging from this point in forward and reverse time are the unperturbed system's homoclinic orbits, denoted Γ^+ and Γ^- in the phase plane diagram of Fig. 5(b). The homoclinic orbits act as impermeable separatrices: A motion of the unperturbed system that starts inside a region enclosed by a separatrix (we refer to that region as a core) remains confined to the core for all time; that is, the motion never escapes

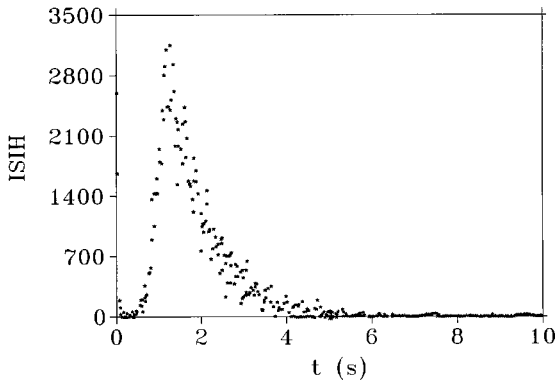

FIG. 4. Interspike interval histogram for the response induced by white noise as simulated by the Fitzhugh-Nagumo equation (after [4]).

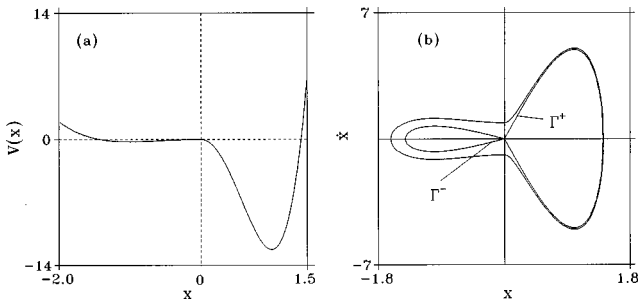

FIG. 5. (a) Potential $V(x)$ [Eq. (7)] ($\alpha_r=49$, $\alpha_l=1$) and (b) phase plane diagram showing homoclinic orbits and an orbit visiting the half planes $x\leqslant 0$ and $x>0$.

from the potential well associated with that core. A motion that starts outside the core remains outside it for all time and visits periodically the two potential wells. An orbit describing such a motion is shown in Fig. 5(b). The homoclinic orbits can be viewed as intersections of the system's stable and unstable manifolds with a plane of section $(x,\dot{x})$. For the unperturbed system the stable and unstable manifolds coincide. The perturbation causes the stable and unstable manifolds to separate. If the Melnikov necessary condition for chaos is satisfied, escapes from a potential well can occur even if the motions start in the perturbed system's counterpart of the core. (As noted earlier, the term ''escapes'' is used in the context of multistable system dynamics and corresponds in this work to the neurophysiological term ''firings.'') We discuss the Melnikov necessary condition for escapes in the next section. For a summary providing additional background and details see, e.g., [7,9].

III. MELNIKOV NECESSARY CONDITION FOR ESCAPES FROM A POTENTIAL WELL

Consider the case where in Eq. (1) the forcing $G(t)$ has the expression

$$G(t)=\sum_{k=1}^{N}\gamma_k\cos(\omega_k t+\varphi_k). \tag{4}$$

The Melnikov necessary condition for chaos, which in this system is also the necessary condition for escapes, is then

$$-\beta 4/3+\gamma_{01}S(\omega_{01})+\gamma_{02}S(\omega_{02})+\sigma\sum_{k=1}^{N}\gamma_k S(\omega_k)>0, \tag{5}$$

where the Melnikov scale factor $S(\omega)$ depends on the potential $V(x)$ [5]. It follows from Eq. (5) that the contribution of a harmonic component to the promotion of chaos, and escapes, depends on frequency via the ordinate of the Melnikov scale factor $S(\omega)$.

If $G(t)$ is a Gaussian stochastic process with unit variance and spectral density $2\pi\Psi_0(\omega)$, then over any finite time interval, however large, it can be approximated as closely as desired by the sum

$$G_N(t)=\sum_{k=1}^{N}\gamma_k\cos(\omega_k t+\varphi_k), \tag{6}$$

where $\gamma_k=\sqrt{2\pi\Psi_0(\omega_k)\Delta\omega}$, $\Delta\omega=\omega_{cut}/N$, $\omega_k=k\Delta\omega$, ω_{cut} is the frequency beyond which the spectrum vanishes or is negligibly small (the cutoff frequency), φ_k is a random variable uniformly distributed in $[0,2\pi]$, and N is finite, albeit large [10]. The Melnikov necessary condition for chaos can then be approximated by an expression with exactly the same form as Eq. (5). It follows from Eq. (6) that, for any given amplitudes γ_{0i} ($i=1,2$) [see Eq. (1)] the respective harmonic functions are less effective in promoting chaos if their frequencies are far from the frequency ω_{pk} of the Melnikov scale factor's peak and the stochastic forcing is similarly less effective if most of the power in the spectrum of the process $G(t)$ is distributed far from ω_{pk} [6]. Like Eq. (5) on which it is based, this statement is, strictly speaking, valid for asymptotically small perturbations. However, as shown, for example, in [11], it remains valid, in a qualitative sense, even if the perturbations are relatively large.

For Eq. (1) chaotic transport into and out of the perturbed system's counterpart of the core can occur only in the half plane $x\leqslant 0$ since owing to the form of Eq. (1) the system remains unperturbed in the half plane $x>0$. This means that the system can exhibit chaotic transport if the Melnikov necessary condition for chaos, Eq. (5), is satisfied for the shallower potential well of Fig. 5(a).

As noted earlier, Eq. (5) shows that an excitation component is more (less) effective in inducing escapes as its frequency is closer to (farther from) the frequency of the peak of the Melnikov scale factor $S(\omega)$. This behavior is similar to the observed behavior summarized by the typical experimental results of Fig. 1. The scale factor $S(\omega)$ for the system should be similar to the bell-shaped response curves of Fig. 1 and its peak should occur at the best frequency indicated by the experiments.

For a given potential $V(x)$, the homoclinic orbits are obtained by integrating Eq. (3) with initial conditions $x=\dot{x}=0$. The scale factor $S(\omega)$, which, as recalled earlier, corresponds to asymptotically small perturbations, is then obtained as the sine transform of the homoclinic orbit's ordinate in the phase plane [12]. However, the inverse operation whereby $V(x)$ is obtained from a given scale factor $S(\omega)$ is considerably more difficult, the more so as in practical applications the perturbation is not asymptotically small. For this reason we need to choose a functional form for $V(x)$ that, with appropriate choices of parameters, yields a scale factor $S(\omega)$ qualitatively similar in shape to the typical response curves of Fig. 1. A reasonably satisfactory model of $V(x)$, which, as is shown subsequently, is qualitatively consistent with the experimental results of [1,2,14], is

$$V(x)=\alpha(x)(-x^2/2+x^4/4), \tag{7}$$

which is a modified version of the Duffing-Holmes potential. In Eq. (7) $\alpha(x)=\alpha_l\approx 1$ for $x\leqslant 0$ and $\alpha(x)=\alpha_r$ for $x>0$, where $\alpha_r\gg\alpha_l$. [It can be verified that $V'(0)=0$.] The potential $V(x)$ is depicted in Fig. 5(a) for $\alpha_r=49$. The Melnikov scale factor corresponding to the left-hand side well of Eq. (7) is

$$S(\omega)=\sqrt{2}\pi\ \mathrm{sech}(\pi\omega/2). \tag{8}$$

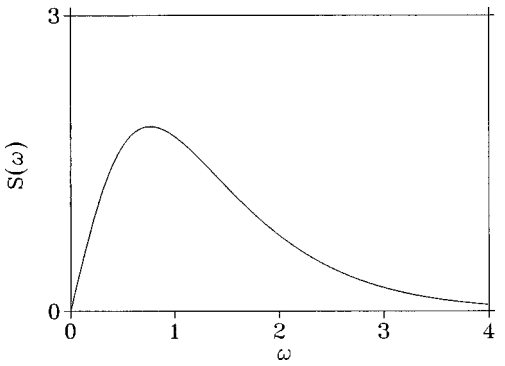

FIG. 6. Melnikov scale factor $S(\omega)$.

Equation (8) is plotted in Fig. 6. Note that the shape of the scale factor of Fig. 6 is qualitatively similar to the shapes of the response curves of Fig. 1. Figure 6 shows that for our model, just as for the experiments of [1], excitation components become increasingly ineffective in inducing chaos (and therefore escapes, i.e., firings) as their frequencies are farther away from a best frequency. This observation originally motivated the choice of the model developed in this work.

Throughout this paper it is assumed that the double-sided spectral density of $G(t)$ is

$$2\pi\Psi_0(\omega)=2\tau/(1+\tau^2\omega^2), \tag{9}$$

in which $\tau=0.02$; that is, the spectral density varies slowly with frequency and is therefore a close approximation of white noise.

IV. CHAOTIC RESPONSE TO HARMONIC AND STOCHASTIC EXCITATION

We now describe a typical chaotic motion pattern for our model. Denote by $\mathcal{R}^-$ the perturbed system's counterpart of the core enclosed by the homoclinic orbit (separatrix) Γ^-. Following an escape from $\mathcal{R}^-$, firing occurs and the motion evolves outside the core enclosed by the impermeable separatrix Γ^+ until its return to the half plane $x\leqslant 0$. Chaotic transport into $\mathcal{R}^-$, followed by another escape (firing), can then occur again. A typical time history of this type of motion is shown in Fig. 7, based on Eq. (1), the potential function of Fig. 5(a), the parameter values $\gamma_{01}=0.11$, $\gamma_{02}=0$, $\beta=0.16$, $\sigma=0.005$, and $\omega_{01}=1.0$, and the spectral density of the process $G(t)$ given by Eq. (9). The weak noise used in the simulations is intended to mimic the noise inducing the fiber's spontaneous activity. As noted in Ref. [1], p. 776, the responses may exhibit multiple firings in response to a harmonic excitation, rather than a single discharge. A double firing can be seen in Fig. 7 at $t/T_{01}\approx 80$.

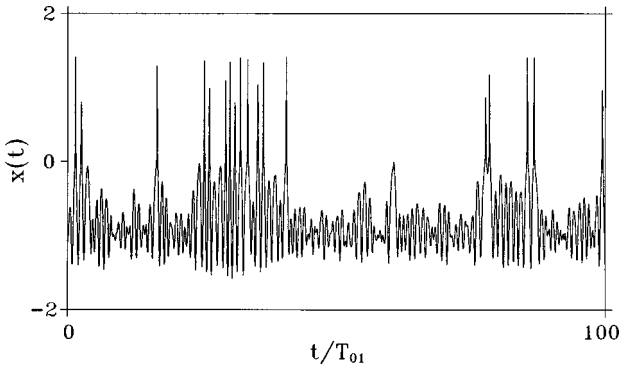

FIG. 7. Time history of the motion induced by harmonic excitation in the presence of noise; see Eq. (1) ($T_{01}=2\pi/\omega_{01}$).

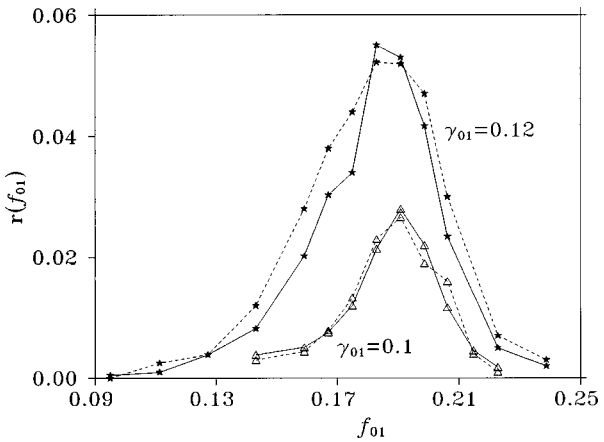

FIG. 8. Dependence of the firing rate r on the harmonic excitation frequency $f_{01}=\omega_{01}/2\pi$ for two excitation amplitudes γ_{01}, simulated by Eq. (1) with harmonic excitation in the presence of noise. Solid and dashed lines correspond to $\alpha_l=1$, $\alpha_r=49$ and $\alpha_l=1$, $\alpha_r=64$, respectively.

The question arises whether our system is robust, i.e., whether its behavior remains qualitatively the same if the parameters of the potential $V(x)$ and the parameter β change within reasonably wide limits corresponding to the parameter region of interest in the experiments. We checked robustness by performing a large number of simulations with $0.95<\alpha_l<1.05$, $45<\alpha_r<64$, and $0.14<\beta<0.3$. In all cases examined the time histories of the responses exhibited no qualitative changes with respect to the time history of Fig. 7. Such changes were observed, however, for parameter values outside these intervals. For example, for $\beta\approx 0.4$ or larger no firings were observed, while for $\beta\approx 0.01$ or smaller the motion consisted only of essentially periodic firings with period close to the harmonic excitation period. We note that the large value of α_r relative to α_l is needed to ensure that the average duration of the spikes is sufficiently small compared

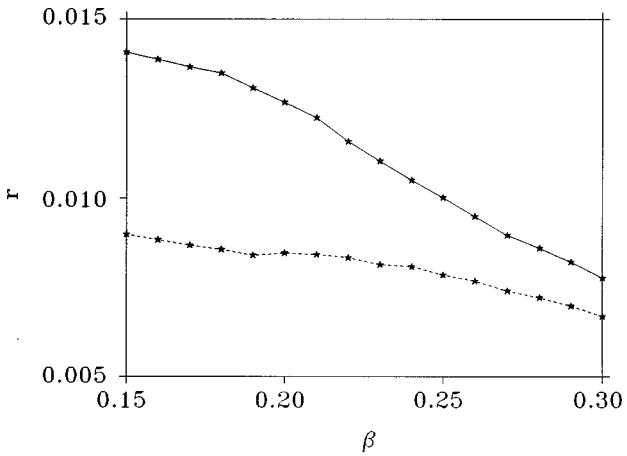

FIG. 9. Dependence of the mean firing rate r on the damping parameter β. Solid and dashed lines correspond to $\gamma_{01}=0.12$ and $\gamma_{01}=0.1$, respectively.

to the average time between firings, as seen in Fig. 7. For additional information on robustness tests see Sec. V.

V. DEPENDENCE OF MEAN FIRING RATE ON FREQUENCY OF HARMONIC EXCITATION

In this section we wish to ascertain that, for finite as opposed to asymptotically small perturbations, the dependence of the model response on the Melnikov scale factor (Fig. 6) is maintained in a qualitative sense and response patterns are therefore similar to those obtained experimentally in [1] (Fig. 1). We assume $\gamma_{02}=0$, $\beta=0.16$, $\sigma=0.005$, and the spectral density of $G(t)$ given by Eq. (9). We show in Fig. 8 the dependence of the mean firing rate r on the frequency ω_{01} for two amplitudes of the harmonic forcing: $\gamma_{01}=0.12$ and $\gamma_{01}=0.10$. For any given frequency, the larger amplitude causes a larger firing rate. For both amplitudes the harmonic excitation is seen to be increasingly ineffective in producing firing as the excitation frequencies are farther away from either end of a relatively narrow best frequency interval. The dependence of the mean firing rate on amplitude and frequency is indeed qualitatively similar to the experimental results of Fig. 1. The results of Fig. 8 are consistent with Melnikov theory only in a qualitative sense as the peak of the Melnikov scale factor (Fig. 6) does not coincide with the peaks of the mean rate plots. This is ascribed to second-order effects resulting from the relatively large perturbation.

We performed checks of the system's robustness also by obtaining from Eq. (1) mean firing rate plots for $\gamma_{01}=0.1$, $\gamma_{0,2}=0.12$, and various excitation frequencies, under the assumption that $\alpha_r=64$, rather than $\alpha_r=49$, all other parameters being unchanged. The results corresponding to these two values are shown in Fig. 8 in interrupted lines and solid lines, respectively.

For $\alpha_r=49$, all other parameters except β being the same as for Fig. 7, we also performed simulations for a number of values $0.14<\beta<0.3$. Results of the simulations are shown in Fig. 9.

VI. INTERSPIKE INTERVAL HISTOGRAMS

We assume again $\gamma_{02}=0$, $\beta=0.16$, $\sigma=0.005$, and the spectral density of $G(t)$ given by Eq. (9). Figures 10(a)–10(c) show ISIH's for $\gamma_{01}=0.12$ and $\omega_{01}=1.25$, $\omega_{01}=1.05$, and $\omega_{01}=0.8$, respectively. The best frequency in this case is $\omega_0\approx 1.1$ (Fig. 6), that is, Figs. 10(a)–10(c) correspond, respectively, to harmonic excitation frequencies higher than, approximately equal to, and lower than the best frequency. The period of the harmonic excitation is $T_{01}=2\pi/\omega_{01}$. The ISIH's of Fig. 10(a)–10(c) were obtained by simulation from Eq. (1). They are multimodal and agree qualitatively with ISIH's based on experiments [2]. Both for the experiments and for Figs. 10(a)–10(c) the peaks in the ISIH's are grouped around the integer multiples of the period of the harmonic excitation. Nevertheless, the firing is aperiodic, which is consistent with the fact that the motions of Figs. 10(a)–10(c) are chaotic even in the absence of noise. The preference for the forcing period and its integer multiples reflects the large spectral ordinate of the response at the forcing frequency (which is typical of the harmonically forced Duffing oscillator; see Ref. [13], p. 88) and the corresponding subharmonics. Note the presence in Fig. 10 of components with periods shorter than the dominant period. As was pointed out in Ref. [1], p. 776, these components reflect the existence of multiple firings.

Like the results of Figs. 10(a)–10(c), ISIH's based on the FHN model [4] are in qualitative agreement with the experimental results of [1]. However, for excitation by nearly white noise the FHN model does not appear to be in agreement with experimental results [2]: The IHIS's obtained from the

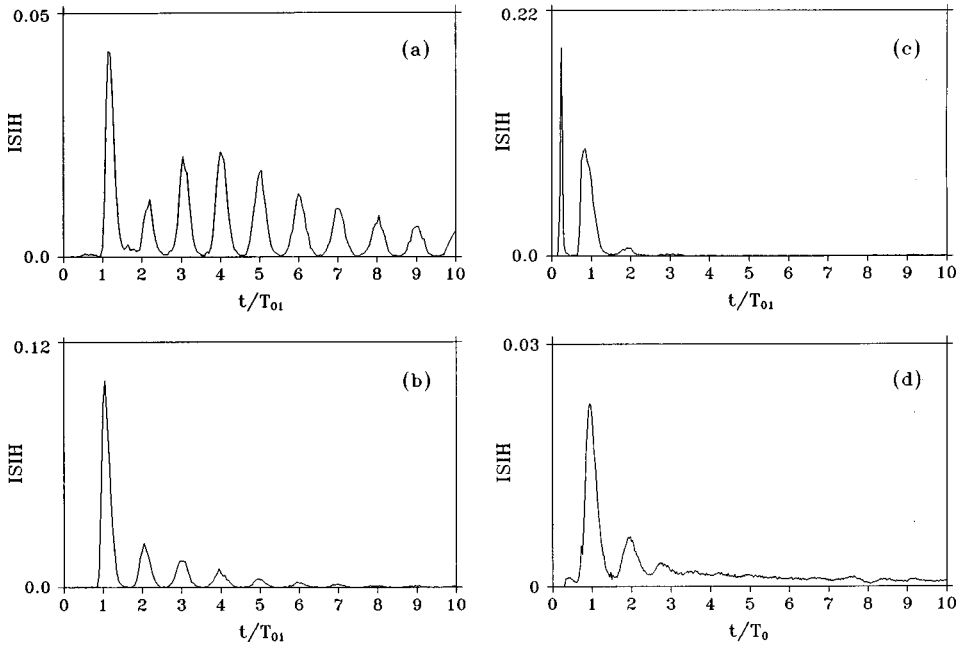

FIG. 10. Interspike interval histograms simulated from Eq. (1): harmonic excitation in the presence of noise for excitation frequency (a) larger than, (b) approximately equal to, and (c) smaller than the best frequency ω_0, and (d) excitation by nearly white noise. T_{01} and T_0 denote the period of the harmonic excitation and the period corresponding to the best frequency, respectively.

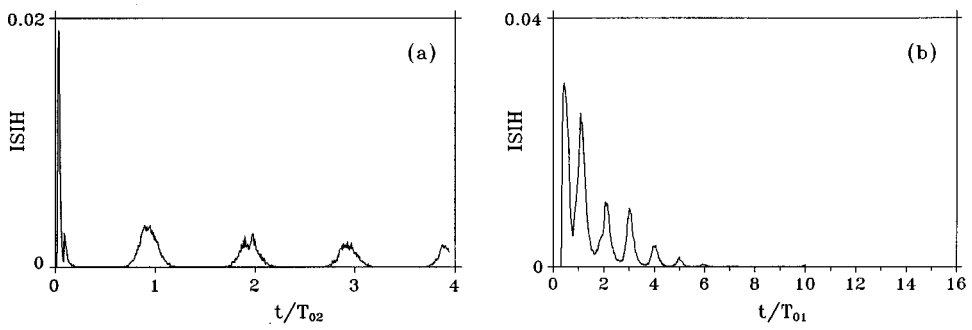

FIG. 11. Interspike interval histograms simulated from Eq. (1) for excitation by two harmonics with frequencies ω_{01} and ω_{02} in the presence of noise. Dominant frequencies are controlled by (a) the component with an inefficient frequency but relatively large amplitude γ_{02} and (b) the component with a frequency ω_{01} close to the best frequency.

experiments are multimodal, whereas those based on the FHN model were found to be unimodal, as shown in Fig. 4 [4]. In contrast, simulations based on the proposed model [see Eq. (1)] agree well with the experimental results of [2]. This is illustrated by Fig. 10(d), which shows a typical ISIH based on Eq. (1) with the same parameters as those of Figs. 10(a)–10(c), except that $\gamma_{01}=0$ and $\sigma=0.035$, that is, the only excitation is stochastic. The ISIH is multimodal with periodicities closely related to the best frequency. The results of Fig. 10(d) are consistent with Melnikov theory since components with the best frequencies (i.e., frequencies closely related to the frequency of the Melnikov scale factor's peak), are the most effective in inducing escapes. The behavior of the system can therefore be expected to be determined by those components and their integer multiples.

Melnikov theory as applied to our model is also in qualitative agreement with results of experiments in which auditory nerve fibers were excited by two harmonic functions in the presence of spontaneous activity [14]. In those experiments the frequency of one of the harmonic excitations, denoted ω_{01}, was close to the best frequency ω_0, while for the second harmonic $\omega_{02}<\omega_0$ so that its effectiveness in inducing firing was relatively weak. The results of [14] indicated that the ISIH are multimodal, with basic period $T_{01}=2\pi/\omega_{01}$ or $T_{02}=2\pi/\omega_{02}$ according to whether the ratio $\eta=\gamma_{01}/\gamma_{02}$ of the amplitudes corresponding to ω_{01} and ω_{02} is relatively large or small. Similar results may be expected for our model, as can be seen from Eq. (5). Even though $S(\omega_{01})$ is larger than $S(\omega_{02})$, if the ratio η is sufficiently small the motion can be dominated by the harmonic with inefficient frequency. That this is indeed the case is shown by the simulations of Figs. 11(a) and 11(b), for which $\omega_{01}=1.0\approx\omega_0$, $\omega_{02}=0.06\ll\omega_0$, $\beta=0.25$, and $\sigma=0.0075$. For Fig. 11(a), $\gamma_{01}=0.01$ and $\gamma_{02}=0.3$ ($\eta=0.033$). Apart from the two peaks at $t/T_{02}\ll 1$, which are ascribed to multiple firings, the spikes are grouped around the period T_{02} and its integer multiples. For Fig. 11(b) $\gamma_{01}=0.1$, $\gamma_{02}=0.16$, and period T_{01} controls.

VII. POTENTIAL FOR STOCHASTIC RESONANCE

Equation (1) describes a bistable system whose unperturbed counterpart, Eq. (3), has homoclinic orbits. It was shown in [9] that such a system has the potential for experiencing stochastic resonance (that is, an increase of the signal-to-noise ratio achieved by *increasing* the noise intensity). That potential exists provided that (i) the signal frequency is sufficiently small in relation to the frequency of the Melnikov scale factor's peak, (ii) in the absence of noise the signal amplitude is too small to bring about chaotic exits from a potential well, and (iii) the intensity of the noise is sufficiently small that the mean escape time induced by the signal and the noise acting together is less than the period of the signal. By adding noise to the excitation the mean escape time is brought in line with the period of the signal. A synchronization effect then occurs wherein the broadband energy associated with the chaotic hopping motion is depleted and transferred to the signal frequency. It is shown in [9] that under certain conditions stochastic resonance may be achieved more effectively by adding to the total excitation a harmonic signal rather than noise. Since, as was pointed out at the beginning of this section, the class of systems studied in [9] includes Eq. (1), all the results of [9] pertaining to stochastic resonance are fully applicable to the model of the auditory nerve fiber proposed in this paper. There appears to be experimental evidence that stochastic resonance is exhibited by some neuronal systems [8]. However, to our knowledge, no stochastic resonance experiments are available on the auditory nerve fiber. We believe, in light of the above remarks, that such experiments would demonstrate that the auditory nerve fiber can indeed experience the stochastic resonance phenomenon.

VIII. CONCLUSIONS

We showed that existing experimental results motivated the use of the stochastic Melnikov approach as a point of departure for constructing a model of the auditory nerve fiber. The proposed model is characterized by a strongly asymmetric double-well potential and allows the use of a novel chaotic dynamics technique, the stochastic Melnikov approach. The model also has an inherent capability for accommodating stochastic resonance phenomena. Numerical simulations showed that the model reproduces qualitatively features of the fiber behavior observed experimentally, including features that appear not to be reproduced by the FHN model. Like the FHN model, our model is entirely phenomenological and its success as a quantitative tool depends upon the choice of appropriate values for its adjustable parameters. Numerical tests confirmed the robustness of the proposed model.

ACKNOWLEDGMENTS

This work was supported in part by the Office of Naval Research, Ocean Engineering Division Grant No. N00014-96-F-0047. Dr. T. Swean served as project monitor.

APPENDIX: DIMENSIONAL COUNTERPART OF TERMS IN EQ. (1)

For the purposes of this appendix it is sufficient to consider the terms $\ddot{x}$ and $\varepsilon(x)\gamma_{01}\cos(2\pi f_{01}t)$ of Eq. (1) ($\omega_{01}=2\pi f_{01}$). Their dimensional counterparts are, respectively, $d^2X/d\tau^2$ and $\varepsilon(X)AP_{01}\cos(2\pi F_{01}t)$, where $X=c_1x$, $\tau=c_2t$, $F=f/c_2$, and X,τ,A have dimensions mV, ms, and mV ms^{-2}, respectively, and P_{01} is expressed in dB. Thus $\gamma_{01}=Ac_2^2P_{01}/c_1$. Our simulations in Figs. 7 and 8 were designed to represent the experimental results of Fig. 1. The scaling factors we used were $c_1=1$ mV (based on the reported amplitudes of the firings of about 1 mV [1]), $c_2=0.183/600$ s$=0.328$ ms (i.e., a nondimensional frequency $f_{01}=0.183$ corresponds to a best frequency of 600 Hz), and $A=0.015$ mV ms^{-2} (i.e., γ_{01} corresponds to $P_{01}=60$ dB). Simulations yielded ratios $\rho=r(f_{01}^{best})/f_{01}^{best}$ of 0.26 and 0.15 for $\gamma_{01}=0.12$ and $\gamma_{01}=0.1$, respectively. For the intermediate value $\gamma_{01}=0.117$ simulations yielded $\rho=0.24$. The corresponding experimental ratios for $P_{01}=70$ dB and $P_{01}=60$ dB are 0.21 and 0.15. The agreement between simulation and experiment is excellent for $\gamma_{01}=0.1$ (corresponding to 60 dB: 0.15 vs 0.15) and fair for $\gamma_{01}=0.117$ (corresponding to 70 dB: 0.21 vs 0.24).

[1] J. R. Rose, J. F. Brugge, D. Anderson, and J. E. Hind, J. Neurophysiol. **30**, 769 (1967).

[2] M. A. Ruggero, J. Neurophysiol. **36**, 569 (1973).

[3] I. J. Hochmair-Desoyer, E. S. Hochmair, H. Motz, and F. Rattay, Neuroscience **13**, 553 (1984).

[4] A. Longtin, J. Stat. Phys. **70**, 309 (1993).

[5] S. Wiggins, *Introduction to Applied Nonlinear Dynamical Systems and Chaos* (Springer-Verlag, New York, 1988).

[6] M. Frey and E. Simiu, Physica D **63**, 321 (1993); E. Simiu and M. Frey, J. Eng. Mech. **122**, 263 (1996).

[7] Y. Sivathanu, C. Hagwood, and E. Simiu, Phys. Rev. E **52**, 4669 (1995).

[8] J. K. Douglass, L. Wilkens, E. Pantazelou, and F. Moss. Nature (London) **365**, 337 (1993); J. E. Levin and J. P. Miller, *ibid.* **380**, 165 (1996); J. J. Collins, T. T. Imhoff, and P. Grigg, J. Neurophysiol. **76**, 642 (1996); P. Cordo, T. Inglis, S. Verschueren, J. J. Collins, D. M. Merfeld, S. Rosenblum, S. Buckley, and F. Moss, Nature (London) **383**, 769 (1996); J. J. Collins, T. Imhoff, and P. Grigg, *ibid.* **383**, 770 (1996).

[9] M. Franaszek and E. Simiu, Phys. Rev. E **54**, 1298 (1996).

[10] S. O. Rice, in *Selected Papers on Noise and Stochastic Processes*, edited by N. Wax (Dover, New York, 1954).

[11] M. Franaszek and E. Simiu, Phys. Lett. A **205**, 127 (1995).

[12] S. Wiggins, *Global Bifurcations and Chaos* (Springer-Verlag, New York, 1990).

[13] J. Guckenheimer and P. Holmes, *Nonlinear Oscillations, Dynamical Systems, and Bifurcations of Vector Fields* (Springer-Verlag, New York, 1990).

[14] J. E. Hind, D. J. Anderson, J. F. Brugge, and J. R. Rose, J. Neurophysiol. **30**, 794 (1967).